Available online at www.sciencedirect.com

SciVerse ScienceDirect

journal homepage: www.elsevier.com/locate/he

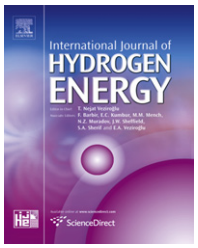

Mesoporous carbon supported PtRu as anode catalyst for direct methanol fuel cell: Polarization measurements and electrochemical impedance analysis of mass transport

Mariano M. Bruno [a,b], *M. Agustina Petruccelli* [a], *Federico A. Viva* [a,*], *Horacio R. Corti* [a,c]

[a] *Grupo Celdas de Combustible, Departamento de Física de la Materia Condensada, Centro Atómico Constituyentes, Comisión Nacional de Energía Atómica (CNEA), Av General Paz 1499 (1650), San Martín, Buenos Aires, Argentina*

[b] *Escuela de Ciencia y Tecnología, Universidad de Gral, San Martín, Martin de Irigoyen 3100 (1650), San Martín, Buenos Aires, Argentina*

[c] *Instituto de Química Física de los Materiales, Medio Ambiente y Energía (INQUIMAE), Facultad de Ciencia Exactas y Naturales, Universidad de Buenos Aires, Intendente Güiraldes 2160 (1428), Ciudad Universitaria, Buenos Aires, Argentina*

ARTICLE INFO

Article history:
Received 6 November 2012
Received in revised form
3 January 2013
Accepted 4 January 2013
Available online 13 February 2013

Keywords:
PtRu catalyst
Mesoporous carbon
Direct methanol fuel cell
Electrochemical impedance spectroscopy
Mass transport

ABSTRACT

The performance of membrane electrode assembly (MEA) prepared with PtRu nanoparticles supported on a mesoporous carbon as anode catalyst are presented and compared against PtRu synthesized over Vulcan carbon. Polarization and power curves were obtained using 1 M methanol aqueous solution at the anode and O_2 at the cathode. The mesoporous carbon supported catalyst shows peak power of 40 mW cm^{-2} and 67 mW cm^{-2} at 30 °C and 60 °C respectively, that is, 15–30% higher than the Vulcan supported catalyst, and exhibits a wider range of operating current. Moreover, an improvement in the mass transport is observed for the catalyst supported on mesoporous carbon, yielding a lower voltage drop at high current density. This behavior was confirmed by electrochemical impedance spectroscopy (EIS), where an increases of the Warburg coefficient value by a factor 3–4 for the catalyst supported on mesoporous carbon as compared with that supported on Vulcan, would indicate a more facile diffusion of methanol through the mesoporous carbon.

1. Introduction

Continuous efforts for improving the performance of Fuel Cell (FC) are of great interest because they hold the promise of a convenient energy source for portable applications, in particular of the Polymer Electrolyte Membrane (PEM) type. Among those type of fuel cells the direct methanol fuel cell (DMFC) has attracted a great deal of attention, partly because of methanol's favorable properties such as high volumetric energy density, ease of handling as a liquid at ambient conditions [1], and also because of the availability of an efficient bimetallic catalyst for methanol oxidation (e.g. PtRu) [2–4]. Nevertheless, noble metals catalysts are required in high loadings to sustain reasonable power densities in DMFC [5,6], not only due to the oxygen reduction reaction on the cathode but also due to methanol oxidation, much more sluggish than H_2 oxidation. The catalyst metal nanoparticles are commonly supported over carbon particles in order to have a good dispersion, increase the

* *Corresponding author*. Tel.: +54 11 6772 7676; fax: +54 11 6772 7121.
E-mail address: viva@tandar.cnea.gov.ar (F.A. Viva).

0360-3199/$ – see front matter
http://dx.doi.org/10.1016/j.ijhydene.2013.01.026

Nomenclature

C_{Adl}	Double layer capacitance (F cm^{-2})
CPE	Constant phase element (Ω cm^2)
j	Current density (mA cm^{-2})
L_k	Relaxation inductance (H cm^{-2})
L_w	Wiring inductance (H cm^{-2})
n_{CPE}	CPE exponential factor
P	Power density (W cm^{-2})
R_{Act}	Anode charge transfer resistance (Ω cm^2)
R_c	Cell resistance (Ω cm^2)
R_{Cct}	Cathode charge transfer resistance (Ω cm^2)
R_k	Relaxation resistance (Ω cm^2)
W	Warburg impedance (Ω cm^2)
$Y_{0\ CPE}$	CPE coefficient (S s^n cm^{-2})
$Y_{0\ W}$	Warburg coefficient (S $s^{0.5}$ cm^{-2})
ω	Frequency (Hz)

surface area and reduce the metal loading as described by numerous reports and reviews on the preparation and characterization on supported catalyst [7–9]. The carbon support also provides the electrical connectivity between the metal particles and the gas diffusion layer or current collector. Carbon blacks, such as Vulcan XC-72, are widely used as catalyst support due to the high electrical conductivity and the surface structure and composition [10–12]. Recently, evidence has demonstrated that the nature of the support and the interaction between support and metal particles affects the morphology, dispersion and stability of the later [13,14] influencing the catalytic activity [9,11,15–20]. Figueiredo et al. [13] observed that the density of oxygen-containing surface groups on carbon supports increased the catalytic activity. Rao et al. [18] analyzed the effect of carbon porosity on the specific activity of the PtRu/C catalyst for methanol oxidation. They found that carbon supports with pores smaller than 20 nm showed poor contact between the metal nanoparticles and Nafion ionomer due to the lack of the ionomer penetration, resulting in a lower methanol oxidation activity.

Over the past few years, mesoporous carbon (MC) with tailored structure has been used as support for fuel cell catalyst exhibiting promising activities both in half cell or single cell configuration [15,21–28]. Joo et al. [21] prepared Pt nanoparticles supported on different ordered mesoporous carbons for fuel cell cathodes and they observed the best catalytic activity for those with small pore size (5 nm). Liu et al. [24] found better electrochemical activity for methanol oxidation, in half cell configuration, by supporting PtRu on different mesoporous carbon as compared to commercial catalyst. Similarly, Arbizzani et al. [15] showed a better performance in a fuel cell configuration of PtRu supported on a mesoporous carbon, obtained by a cryogel method, as compared to the catalyst supported on Vulcan. Controlling the structural parameters, such as surface area, pore size and particle morphology, provides extra fine tuning of the catalyst electroactivity [8,10,11,29]. Moreover, porous carbons have shown to allow the preparation of highly dispersed catalytic nanoparticles, exhibiting good diffusion properties for reactants and by-products [8,30–32]. In contrast, carbon powders like Vulcan XC-72 with a much simple particle structure and lower surface area might not provide the best substrate for metal particles.

Recently we reported the electrochemical characterization of PtRu nanoparticles deposited on mesoporous carbon (PtRu/MC) [33,34]. The electrochemical measurements showed that the PtRu/MC presented a 25% increase of the methanol oxidation current compared to the PtRu supported on carbon Vulcan. In cyclic voltammetry experiments a lower onset potential for the oxidation of methanol was observed for PtRu/MC, and a lower poisoning rate was also confirmed from the chronoamperometry analysis. Differential electrochemical mass spectroscopy (DEMS) showed a methanol to CO_2 current efficiency conversion for PtRu/MC 8% higher as compared to the Vulcan supported catalyst (PtRu/C).

Electrochemical impedance spectroscopy (EIS) has been demonstrated to be a powerful technique for the analysis of the several physicochemical processes taking place inside a PEMFC [35–38]. The EIS analysis of PEMFC, presented commonly as a Nyquist plot (real impedance vs. imaginary impedance), could exhibit up to three arcs depending on the measurements conditions [35,39–41]. The system is usually modeled through an equivalent circuit composed by a combination of electrical elements, allowing the description of the different processes taking place inside the fuel cell [42,43].

In the present work we describe the fuel cell characterization of the aforementioned PtRu catalyst, prepared by the impregnation-reduction method, supported on a high surface area mesoporous carbon [33]. Fuel cell measurements were performed on a single MEA cell having 5 cm^2 active area with 1 M methanol used as anode fuel and dry O_2 on the cathode. Electrochemical impedance spectroscopy was performed on working fuel cell at different cell voltages focusing on the mass transport properties of the mesoporous carbon supported catalyst. The EIS response was fitted with an equivalent circuit with the aim to assess the characteristics of the methanol diffusion in the fuel cell.

2. Experimental

2.1. *Mesoporous carbon and catalyst supported preparation*

Mesoporous carbon support was obtained using the method previously described [44,45]. Briefly, a precursor was prepared by polymerization of resorcinol (Fluka) and formaldehyde (Cicarelli, 37 wt%). Sodium Acetate (Cicarelli) was used as catalyst and a cationic polyelectrolyte (polydilayl- dimethylammonium chloride, PDADMAC, Sigma–Aldrich) was used as a structuring agent. The carbonized material at 1000 °C was grinded and passed through a mesh with a pore size of 40 μm. The mesoporous carbon had a surface area of 580 m^2 g^{-1} as obtained by BET, and the pore size distribution shows a peak at 20 nm.

The preparation and characterization of PtRu nanoparticles on MC and Vulcan was described elsewhere [33]. Briefly, adequate amounts of solutions of the metal precursors $H_2PtCl_6 \cdot 6H_2O$ (Tetrahedron) and $RuCl_3 \cdot 3XH_2O$ (Aldrich) were added to a slurry of the carbon support while stirring. The pH

was adjusted to 8 with 1 M NaOH (Pro Analysis, Merck) aqueous solution and heated to 80 °C $NaBH_4$ (granular 98%, Sigma–Aldrich) was added in a molar ratio of 3:1 ($NaBH_4$ to metal salt) to the suspension while heating for 2 h, followed by stirring for 12 h at room temperature. The liquid was centrifuged and the solid was separated, washed and dried on a vacuum oven at 60 °C overnight. The obtained PtRu/MC had a 62% metal loading with 4.0 nm mean particle diameter while for PtRu/C the values were 58% and 5.0 nm, respectively, as obtained by thermogravimetric analysis (TG), X-ray diffraction (XRD), energy dispersive X-ray spectroscopy (EDS) and transmission electron microscopy (TEM) [33].

2.2. MEA preparation and fuel cell testing

PtRu/MC and PtRu/C were used as anode catalyst while Pt/C 60% (Fuel Cell Store) was used as cathode catalyst. The catalyst suspension was prepared by mixing the catalyst with milli-Q water and Nafion ionomer solution (5%, Ion Power) in a 1:3:1 proportion by weight, and spread on one side of a 5 cm^2 Toray C paper TGP–H 60 10% PTFE coated (Fuel Cell Technologies), for a final electrode loading *ca.* 3 mg cm^{-2}. A Nafion 212 membrane (Ion Power) was placed in between the electrodes and hot pressed at 150 °C and 40 bar for 25 min. The Nafion membrane was previously treated by boiling in H_2O_2 3% (H_2O_2 30%, Biopack) followed by H_2SO_4 3% (95–97%, Merck). The MEAs were mounted in a standard single cell housing with pin-type flow fields (Fuel Cell Technologies, Inc.). Proper Teflon gasket films (50–150 um) were inserted and the cell uniformly bolted with a torque of 2.3 N m. After assembly of the cell, the MEA was rehumidify by circulating water overnight at 80 °C. Galvanodynamic polarization test was performed at two different temperatures (30 °C and 60 °C) from the open circuit voltage (OCV) to a voltage close of short circuit (0.05 V) while circulating 1 M methanol (Merk, HPLC grade) through the anode and dry O_2 (RG 4.8, Indura) through the cathode. A Gilson Minipuls 3 peristaltic pump was used to circulate the methanol solution and a digital mass flow meter MC 200 from Alicat Scientific to control the O_2 flows. For all the measurements the methanol flow was set to 2.0 ml min^{-1} while the O_2 flow was 200 sccm leading a methanol to O_2 stoichiometry ratio of 1:4.

Electrochemical impedance spectroscopy measurements were performed on the FC in the working mode. The working (WE) and sensing electrode (SE) leads were connected to the fuel cell anode and those corresponding to the counter (CE) a reference electrode (RE) to the cathode [40]. The measurements were performed at three different voltages (0.20 V, 0.15 V and 0.10 V) chosen so that the cell operates in the high current density zone, at 60 °C. Frequencies were swept from 100 kHz to 100 mHz with 10 mV amplitude.

All measurements were performed with an Autolab PGSTAT302N potentiostat equipped with a 20 A booster.

3. Results and discussion

3.1. Fuel cell test

Polarization measurements at 30 °C and 60 °C for the fuel cells with PtRu/MC and PtRu/C as anode catalyst are shown in Fig. 1(A, B). Both catalysts show similar values for the OCV at each temperature (*ca.* 0.65 V). The initial drop in voltage on the activation polarization zone is also similar for both catalysts at each temperature indicating a comparable charge transfer resistance.

The main differences between the catalysts arise as the current density increases. Above 100 mA cm^{-2} at 30 °C and 200 mA cm^{-2} at 60 °C the voltage of PtRu/MC remains higher than that of PtRu/C. Therefore, the limiting current density value for PtRu/MC is higher than that of PtRu/C at both temperatures. Such behavior traduces in a higher power output for PtRu/MC being 40 mW cm^{-2} and 67 mW cm^{-2} at 30 °C and 60 °C, respectively. Table 1 shows the values of the current density (j) and power density (P) at 0.4 V and the limiting current (j_{lim}) and peak power density (P_{peak}) for both catalysts at each temperature. The values for j and P are also presented by grams of Pt in order to emphasize the utilization of Pt in the catalyst. Fig. 2 shows the polarization and power plots for PtRu/MC at 30 °C and 60 °C with the current and power expressed by mass (in grams) of Pt. The polarization curves indicate an overall better performance for PtRu/MC compared to PtRu/C, especially in the mass transport controlled region.

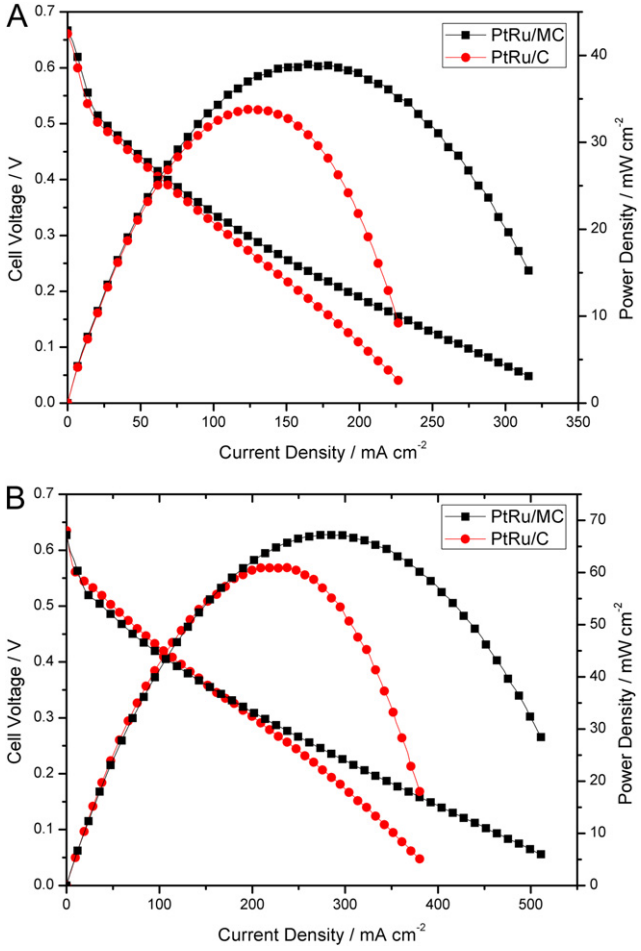

Fig. 1 – Polarization and power curves for PtRu/MC and PtRu/C with 1 M methanol and dry O_2 (200 sccm). A) 30 °C, B) 60 °C.

Table 1 – Current density and power density per area and per gram of Pt at 0.4 V, and at the characteristic limiting current (j_{lim}) and peak power (P_{peak}).

	PtRu/C		PtRu/MC	
	30 °C	60 °C	30 °C	60 °C
j (mA cm^{-2})	62	117	65	111
j (A g_{Pt}^{-1})	41	60	46	74
P (mW cm^{-2})	25	47	26	44
P (W g_{Pt}^{-1})	16	24	18	30
j_{lim} (mA cm^{-2})	230	380	320	510
j_{lim} (A g_{Pt}^{-1})	150	190	210	340
P_{peak} (mW cm^{-2})	34	61	39	67
P_{peak} (W g_{Pt}^{-1})	17	31	26	45

3.2. *Fuel cells EIS measurements*

A typical FC polarization curve presents three well defined zones [46]. Fig. 3 shows the shape of the polarization curve obtained from a semi-empirical equation describing the well known zones, activation polarization (zone 1), ohmic polarization (zone 2) and mass transport polarization (zone 3) [47].

The polarization plots (Fig. 1A and B) obtained for both catalysts exhibit the shape of the theoretical curve shown in Fig. 3, with differences at high current density, where the system is under mass transport control. While PtRu/C shows the characteristic decrease in voltage, the PtRu/MC maintains the j vs. V slope of the ohmic polarization zone, indicating better methanol diffusion at both temperatures. In order to show more clearly this behavior, the derivative of the polarization for both fuel cells at 60 °C are presented in Fig. 4, which can be compared to the derivative of the theoretical polarization plot, presented in Fig. 3 inset. Both catalysts exhibit, in the zone 1 and 2, a response similar to the theoretical graph. However, for j above 200 mA cm^{-2}, the observed voltage derivative decline for PtRu/C, probably because of a deficient methanol mass transport as compared to the PtRu/MC, which maintains the slope value.

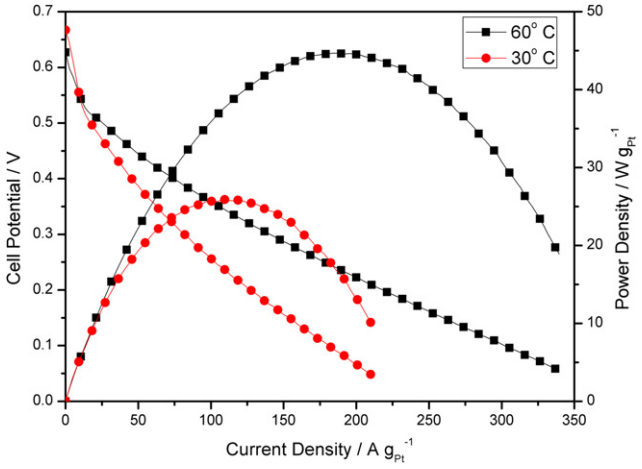

Fig. 2 – Polarization and power curves for PtRu/MC with 1 M methanol and dry O_2 (200 sccm) at 30 °C and 60 °C with the current and power expressed by gram of Pt.

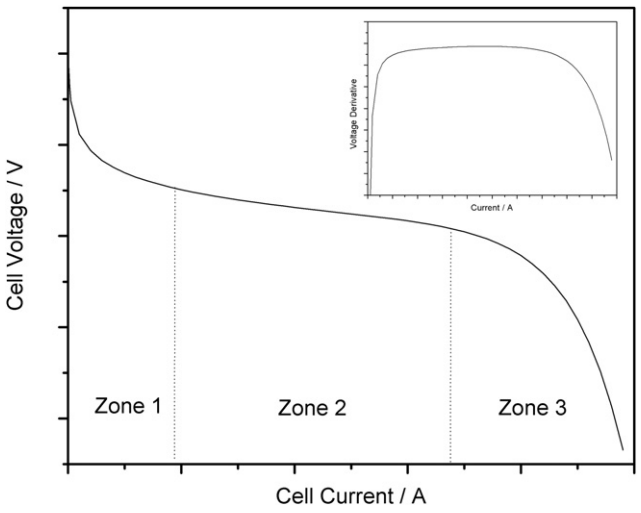

Fig. 3 – Theoretical form of the fuel cell polarization plot. Zone 1: Activation polarization. Zone 2: Ohmic polarization. Zone 3: Mass transport polarization. Inset: Derivative of the voltage vs. the current.

We proposed in a previous work that the mesoporous carbon is a better support for the PtRu catalyst because it enhances the mass transport processes as was observed by the electrochemical analysis [33]. In order to further analyze the behavior observed in the polarization curves, EIS experiments were conducted in the working fuel cell at voltages corresponding to high current densities. Fig. 5(A, B) shows the Nyquist plots for both catalyst at three different voltages, corresponding to the mass transport zone. The lines representing the fits were obtained with the equivalent circuit shown in Fig. 6. This circuit was used by Wagner and coworkers to explain the CO anode poisoning effect in PEMFC [48,49]. That circuit provided the best fit of the impedance spectra in comparison to other circuits used for DMFC [36,39], as can be observed by the good correlation between the data and the fitted curves, and supported by the low value obtained

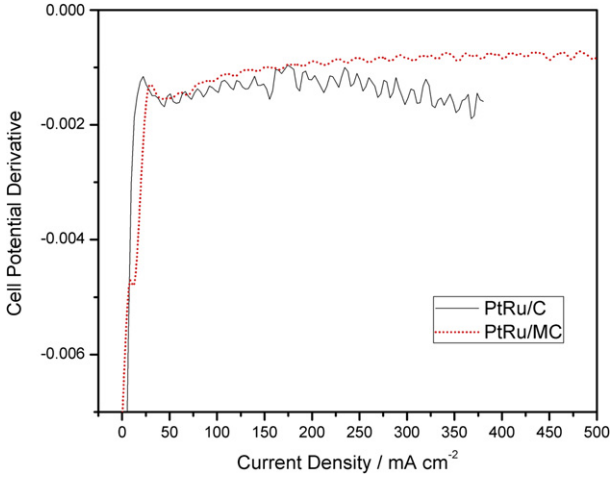

Fig. 4 – Derivative of the polarization plot for PtRu/MC and PtRu/C at 60 °C.

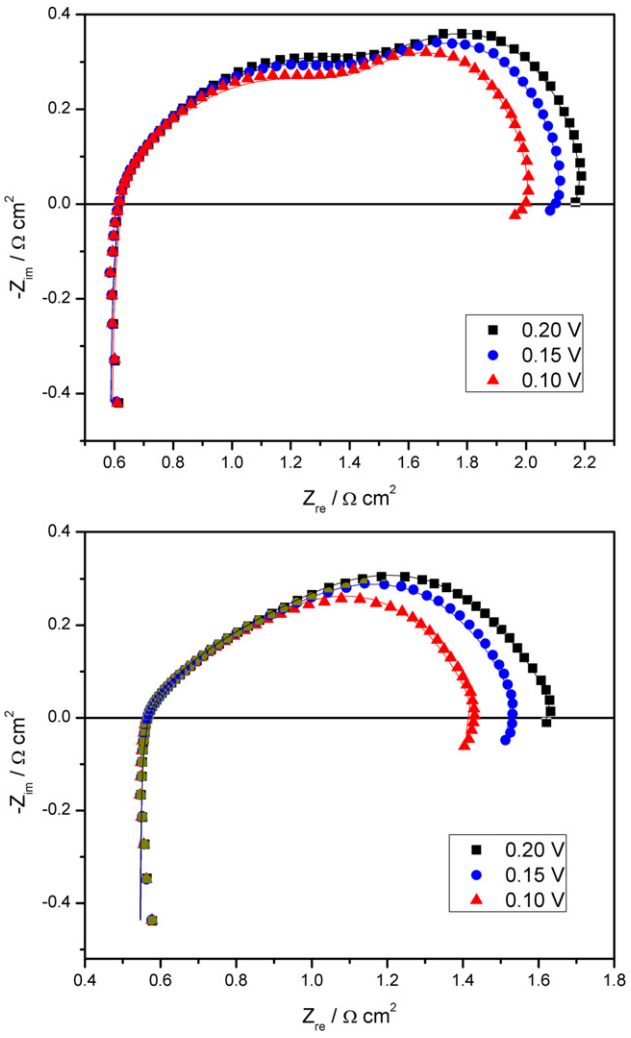

Fig. 5 – Nyquist plot at three different voltages for the fuel cell at 60 °C. A) PtRu/MC, B) PtRu/C. The lines correspond to the fit by the equivalent circuit.

for the statistical dispersion. A possible explanation for the optimal fit obtained with the mentioned circuit might be due to the high amount of CO formed at high current densities, which presents a significant poisoning effect. The equivalent circuit shows the common elements found for a fuel cell [37], namely, the cell resistance (R_c), the charge transfer resistance for the anode (R_{Act}) and the cathode (R_{Cct}) and the anode double layer capacitance (C_{Adl}). In series with the cell resistance a parasitic wiring inductance (L_w) related to the mutual induction effect of the cell and the connection wires is present [37,50]. The inductance fits the observed positive Z_{im} at very high current density in both graphs. In the anode side, the circuit presents a relaxation resistance (R_k) in series with a relaxation inductance (L_k), which constitutes a surface relaxation impedance [48,49] describing relaxation processes at the electrode interface and used to fit the pseudo-inductive behavior observed at low frequencies. Such impedance may be originated from the catalyst CO poisoning due to methanol incomplete oxidation in DMFC [39,51], *vide infra*. In series with the anode charge transfer resistance there is a Warburg impedance (W) describing the mass transport processes. In the cathode side of the circuit, R_{Cct} is in parallel with a constant phase element (CPE) that fits the double layer capacitance of the cathode better than the simple capacitor model [37,39].

Table 2 shows the results for the different elements composing the equivalent circuit obtained by fitting the EIS data. The cell resistance values are quite similar for both cells. This indicates the reproducibility of the MEAs preparation method in terms of the ink formulation and hot-pressing conditions. Moreover, L_w has similar values for both cells, consistent with the fact that the same system, including the cell, was used in all measurements. R_{Act} and R_{Cct} also show similar values for each catalyst, as expected from the similar initial drop in the polarization curves. C_{Adl} for PtRu/MC is almost twice to the one observed for PtRu/C, a result also expected since the MC surface area is more than double than that of carbon Vulcan.

The values of R_k and L_k reported in Table 2 for the PtRu/C indicate a higher value for the relaxation time constant τ_k (L_k/R_k) [48,49], as observed by the inductive loop at the low frequency end of the Nyquist plot (Fig. 5B). As mentioned above, the use of R_k and L_k was carried out by Wagner and co-workers to explain the CO poisoning effects in PEMFC anodes. These authors concluded that a higher value of the relaxation time constant indicated a higher CO poisoning [48,49]. In the present work the use of the R_k and L_k was necessary to fit the pseudo-inductive behavior observed at low frequencies. A plausible explanation in a DMFC could be the presence of CO

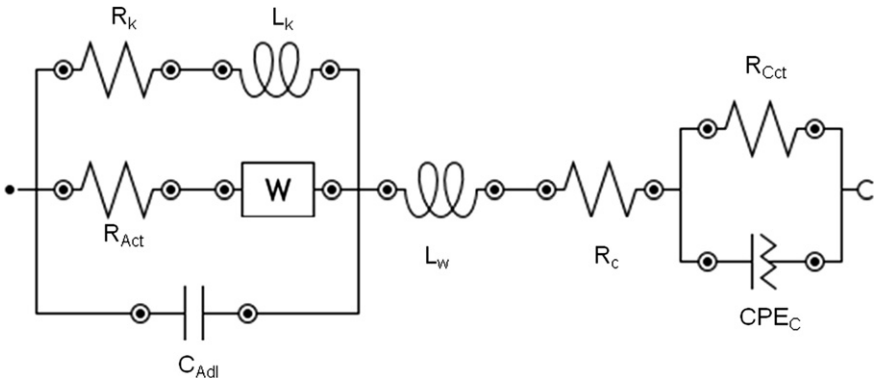

Fig. 6 – Equivalent circuit used to fit the DMFC Nyquist plots.

Table 2 – Values for the equivalent circuit elements obtained by fitting the Nyquist plots at 60 °C.

Voltage V		R_k $\Omega\ cm^2$	L_k $H\ cm^{-2}$	R_{Act} $\Omega\ cm^2$	$Y_{0\ W}$ $S\ s^{0.5}\ cm^{-2}$	C_{Adl} $F\ cm^{-2}$	R_c $\Omega\ cm^2$	L_w $H\ cm^{-2}$	R_{Cct} $\Omega\ cm^2$	$Y_{0\ CPE}$ $S\ s^n\ cm^{-2}$	n_{CPE}
0.20	PtRu/MC	1.74	4.16E-08	0.433	96.2	0.089	0.654	1.93E-08	1.23	7.4	0.552
	PtRu/C	0.50	4.36E-08	0.272	31.0	0.059	0.54	2.82E-08	0.83	21.65	0.528
0.15	PtRu/MC	1.38	4.00E-08	0.416	110.0	0.092	0.654	1.93E-08	1.17	7.2	0.558
	PtRu/C	0.38	4.60E-08	0.287	31.6	0.075	0.54	2.82E-08	0.74	20.1	0.541
0.10	PtRu/MC	1.32	3.83E-08	0.416	114.0	0.090	0.654	1.93E-08	1.05	7.1	0.555
	PtRu/C	0.16	5.06E-08	0.265	30.4	0.051	0.54	2.82E-08	0.64	16.95	0.559

due to incomplete methanol oxidation. As it is well known, PtRu is the best catalyst for methanol oxidation due to the so called bifunctional mechanism, where Pt oxidizes methanol to CO, and OH groups adsorbed on a neighboring Ru site oxidizes the CO to CO_2 [52]. However, not all nanoparticles possess the same PtRu atomic ratio, therefore could be Pt sites without a neighboring Ru sites resulting in the catalyst partial poisoning by CO [52]. Such behavior will be more noticeable at high current densities where the oxidation rate is higher. As was shown previously by DEMS analysis [33], the PtRu/MC catalyst has a higher rate of methanol oxidation to CO_2 than PtRu/C and therefore lower poisoning rate which results in a lower τ_k as compared to PtRu/C.

The depression of the semicircle at the high frequency end in the Nyquist plot was attributed by several authors as a coupling of interfacial and diffusional impedance [35,36,39], and also to the roughness of highly dispersed electrodes surfaces [53]. The use of the Warburg element in the circuit of Fig. 6 was essential to fit the semicircle depression, which is more noticeable in the case of PtRu/C (Fig. 5B). Table 2 shows the Warburg coefficient ($Y_{0\ W}$) [43] values for both catalyst at the different voltages. This coefficient is three to four times higher for PtRu/MC than for PtRu/C, indicating that the impedance is higher for the later at each individual frequency, as can be deduced from eq. (1).

$$W = \frac{1}{Y_{0\ W}\sqrt{j\omega}} \tag{1}$$

As it was mentioned in Section 2.2, the stoichiometry conditions of the measurements were set in order that the cathode reaction would not provide a limiting factor. Therefore, the variation in mass transport behavior between the two cells can be assigned to the carbon support. The difference in the $Y_{0\ W}$ values for both catalysts is an indication of faster methanol diffusion in PtRu/MC compared to PtRu/C. On the other hand, the mass transport phenomena also affects the low frequency semicircle [36]. For PtRu/MC the impedance in the Nyquist plot at low frequency is higher than for PtRu/C. A plausible explanation is that the cathode impedance plays a predominant role in the MC supported catalyst, since a higher amount of methanol is being oxidized at the measured potentials (Fig. 1). Nevertheless, the semicircle depression is highly noticeable in the PtRu/C and the value of $Y_{0\ W}$ obtained for PtRu/MC is indicative of a less hindered mass transport, agreeing with the behavior presented in the polarization curve, and also with the electrochemical measurements previously reported [33].

4. Conclusions

The characterization of a PtRu catalyst supported on a mesoporous carbon in a fuel cell and the comparison with the same catalyst supported on carbon Vulcan was performed. Polarization and power curves indicate a better performance of the mesoporous supported catalyst at 30 °C and 60 °C as compared to the one supported on Vulcan, yielding a peak power of 67 mW cm^{-2} or 45 W gr_{Pt}^{-1} at 60 °C. Moreover, it was observed that the methanol mass transport at high current densities, where the mass transport dominates the polarization curve, is less restricted in the cell with PtRu/MC than in the PtRu/C cell. Such behavior was further analyzed by EIS where the Warburg coefficients indicated a better mass transport in the mesoporous carbon as compared to Vulcan. These results, together with the ones showed in our previous report, indicate that the MC due to its morphology is a better support for PtRu than Vulcan in terms of catalyst performance and mass transport as shown by the polarization plots and EIS results.

The low frequency semicircle for PtRu/MC in the Nyquist plot showed a behavior that will be the subject of a future study.

Acknowledgments

The authors thank financial support from Agencia Nacional de Promoción Científica y Tecnológica (ANPCyT) (PICT 0008-2009 PRH 200-4, PICT 2097), CONICET (PIP 00095) and UNSAM SJ10/04. MMB, FAV and HRC are permanent research fellows of CONICET.

REFERENCES

[1] Edlund D. Methanol fuel cell systems: advancing towards commercialization. 1st ed. Pan Stanford Publishing; 2011.
[2] Jansen MMP, Moolhuysen J. Binary systems of platinum and a second metal as oxidation catalysts for methanol fuel cells. Electrochim Acta 1976;21(1):869–78.
[3] Surampudi S, Narayanan SR, Vamos E, Frank H, Halpert G, Laconti A, et al. Advances in direct oxidation methanol fuelcells. J Power Sources 1994;47(3):377–85.
[4] Watanabe M, Uchida M, Motoo S. Preparation of highly dispersed Pt + Ru alloy clusters and the activity for the electrooxidation of methanol. J Electroanal Chem 1987; 229(1–2):395–406.
[5] Carrette L, Friedrich KA, Stimming U. Fuel cells: principles, types, fuels, and applications. Chem Phys Chem 2000;1:162–93.

[6] Arico AS, Baglio V, Antonucci V. Direct methanol fuel cells. Energy science, engineering and technology series. New York: Nova Science Publishers, Inc; 2010.
[7] Lizcano Valbuena WH, de Azevedo DC, Gonzalez ER. Supported metal nanoparticles as electrocatalysts for low-temperature fuel cells. Electrochim Acta 2004;49(8):1289–95.
[8] Liu H, Song C, Zhang L, Zhang J, Wang H, Wilkinson D. A review of anode catalysis in the direct methanol fuel cell. J Power Sources 2006;155:95–110.
[9] Cui Z, Liu C, Liao J, Xing W. Highly active PtRu catalysts supported on carbon nanotubes prepared by modified impregnation method for methanol electro-oxidation. Electrochim Acta 2008;53(27):7807–11.
[10] Auer E, Freund A, Pietsch J, Tacke T. Carbons as supports for industrial precious metal catalysts. Appl Catal A 1998;173: 259–71.
[11] Pantea D, Darmstadt H, Kaliaguine S, Roy C. Electrical conductivity of conductive carbon blacks: influence of surface chemistry and topology. Appl Surf Sci 2003;271: 181–93.
[12] Pantea D, Darmstadt H, Kaliaguine S, Summchen L, Roy C. Electrical conductivity of thermal carbon blacks: influence of surface chemistry. Carbon 2001;39:1147–58.
[13] Figueiredo J, Pereira M, Serp P, Kalck P, Samant P, Fernandes J. Development of carbon nanotube and carbon xerogel supported catalysts for the electro-oxidation of methanol in fuel cells. Carbon 2006;44(12):2516–22.
[14] Zhou WJ, Li WZ, Song SQ, Zhou ZH, Jiang LH, Sun GQ, et al. Bi- and tri-metallic Pt-based anode catalysts for direct ethanol fuel cells. J Power Sources 2004;131(1–2):217–23.
[15] Arbizzani C, Beninati S, Soavi F, Varzi A, Mastragostino M. Supported PtRu on mesoporous carbons for direct methanol fuel cells. J Power Sources 2008;185(2):615–20.
[16] Gomez de la Fuente JL, Martinez Huerta MV, Rojas S, Terreros P, Fierro JLG, Peña MA. Methanol electrooxidation on PtRu nanoparticles supported on functionalised carbon black. Catal Today 2006;116:422–32.
[17] Kim H, You D, Yoon H, Joo S, Pak C, Chang H, et al. Cathode catalyst layer using supported Pt catalyst on ordered mesoporous carbon for direct methanol fuel cell. J Power Sources 2008;180(2):724–32.
[18] Rao V, Simonov P, Savinova E, Plaksin G, Cherepanova S, Kryukova G, et al. The influence of carbon support porosity on the activity of PtRu/Sibunit anode catalysts for methanol oxidation. J Power Sources 2005;145:178–87.
[19] Uchida M, Fukuoka Y, Sugawara Y, Eda N, Ohta A. Effects of microstructure of carbon support in the catalyst layer on the performance of polymer-electrolyte fuel cells. J Electrochem Soc 1996;143(7):2245–52.
[20] Uchida M, Fukuoka Y, Sugawara Y, Ohara H, Ohta A. Improved preparation process of very-low-platinum-loading electrodes for polymer electrolyte fuel cells. J Electrochem Soc 1998;145(11):3708–13.
[21] Joo SH, Lee HI, You DJ, Kwon K, Kim JH, Choi YS, et al. Ordered mesoporous carbons with controlled particle sizes as catalyst supports for direct methanol fuel cell cathodes. Carbon 2008;46:2034–45.
[22] Joo SH, Pak C, You DJ, Lee S-A, Lee HI, Kim JM, et al. Ordered mesoporous carbons (OMC) as supports of electrocatalysts for direct methanol fuel cells (DMFC): effect of carbon precursors of OMC on DMFC performances. Electrochim Acta 2006;52:1618–26.
[23] Lei Z, Bai S, Xiao Y, Dang L, An L, Zhang G, et al. CMK-5 mesoporous carbon synthesized via chemical vapor deposition of ferrocene as catalyst support for methanol oxidation. J Phys Chem C 2008;112:722–31.
[24] Liu SH, Yu WY, Chen CH, Lo AY, Hwang BJ, Chien SH, et al. Fabrication and characterization of well-dispersed and highly stable PtRu nanoparticles on carbon mesoporous material for applications in direct methanol fuel cell. Chem Mater 2008;20:1622–8.
[25] Zhou JH, He JP, Ji YJ, Dang WJ, Liu XL, Zhao GW, et al. CTAB assisted microwave synthesis of ordered mesoporous carbon supported Pt nanoparticles for hydrogen electro-oxidation. Electrochem Solid State Lett 2007;10:B191–5.
[26] Ding J, Chana KY, Rena J, Xiao FS. Platinum and platinum–ruthenium nanoparticles supported on ordered mesoporous carbon and their electrocatalytic performance for fuel cell reactions. Electrochim Acta 2005;50:3131–41.
[27] Ambrosio EP, Dumitrescu MA, Francia C, Gerbaldi C, Spinelli P. Ordered mesoporous carbons as catalyst support for PEM fuel cells. Fuel Cells 2009;9(3):197–200.
[28] Wikander K, Ekström H, Palmqvist AEC, Lundblad A, Holmberg K, Lindbergh G. Alternative catalysts and carbon support material for PEMFC. Fuel Cells 2006;6(1):21–5.
[29] Bruno MM, Cotella NG, Miras MC, Koch T, Seidler S, Barbero C. Characterization of monolithic porous carbon prepared from resorcinol/formaldehyde gels with cationic surfactant. Colloids Surf A 2010;358:13–20.
[30] Sahu AK, Sridhar P, Pitchumani S. Mesoporous carbon for polymer electrolyte fuel cell electrodes. J Indian Inst Sci 2009; 89:437–45.
[31] Bruno MM, Franceschini EA, Planes GA, Corti HR. Electrodeposited platinum catalysts over hierarchical carbon monolithic support. J Appl Electrochem 2010;40(2):257–63.
[32] Bruno MM, Corti HR, Balach J, Cotella GN, Barbero CA. Hierarchical porous materials: capillaries in nanoporous carbon. Funct Mat Lett 2009;2:135–8.
[33] Viva FA, Bruno MM, Jobbagy M, Corti HR. Electrochemical characterization of PtRu nanoparticles supported on mesoporous carbon for methanol electrooxidation. J Phys Chem C 2012;116:4097–104.
[34] Viva FA, Bruno MM, Corti HR. Mesoporous carbon as support for PtRu catalyst. Electrochemical and fuel cell characterization. ECS Trans 2011;41:1121–30.
[35] Mueller JT, Urban PM. Characterization of direct methanol fuel cells by ac impedance spectroscopy. J Power Sources 1998;75:139–43.
[36] Mueller JT, Urban PM, Holderich WF. Impedance studies on direct methanol fuel cell anodes. J Power Sources 1999:157–60.
[37] Wagner N. Fuel cells. In: Barsoukov E, Macdonald JR, editors. Impedance spectroscopy: theory, experiment, and applications. New Jersey: Wiley; 2005. p. 497–530.
[38] Yuan X, Wang H, Colinsun J, Zhang J. AC impedance technique in PEM fuel cell diagnosis—a review. Int J Hydrogen Energ 2007;32(17):4365–80.
[39] Hsu NY, Yen SC, Jeng KT, Chien CC. Impedance studies and modeling of direct methanol fuel cell anode with interface and porous structure perspectives. J Power Sources 2006; 161(1):232–9.
[40] Yang SH, Chen CY, Wang WJ. An impedance study of an operating direct methanol fuel cell. J Power Sources 2010; 195(8):2319–30.
[41] Xue X, Bock C, Birry L, MacDougall BR. The influence of Pt loading, support and Nafion content on the performance of direct methanol fuel cells: examined on the example of the cathode. Fuel Cells 2011;11(2):286–300.
[42] Macdonald JR, Johnson WB. Fundamentals of impedance spectroscopy. In: Barsoukov E, Macdonald JR, editors. Impedance spectroscopy: theory, experiment, and applications. New Jersey: Wiley; 2005. p. 1–20.
[43] Orazem ME, Tribollet B. Electrochemical impedance spectroscopy. New Jersey: John Wiley & Sons; 2008.
[44] Bruno MM, Cotella Nelson G, Miras MC, Barbero C. A novel way to maintain resorcinol–formaldehyde porosity during

drying: stabilization of the sol–gel nanostructure using a cationic polyelectrolyte. Colloids Surf A 2010;362:28–32.
[45] Ramos-Sánchez G, Bruno MM, Thomas YRJ, Corti HR, Solorza-Feria O. Mesoporous carbon supported nanoparticulated PdNi2: a methanol tolerant oxygen reduction electrocatalyst. Int J Hydrogen Energ 2012;37(1): 31–40.
[46] Barbir F. PEM fuel cells: theory and practice. 1st ed. Academic Press; 2005.
[47] Yuan XZ, Wang H. In: Zhang J, editor. PEM fuel cell electrocatalysts and catalyst layers. London: Springer; 2008. p. 1–79.
[48] Wagner N, Gülzow E. Change of electrochemical impedance spectra (EIS) with time during CO-poisoning of the Pt-anode in a membrane fuel cell. J Power Sources 2004;127(1–2): 341–7.
[49] Wagner N, Schulze M. Change of electrochemical impedance spectra during CO poisoning of the Pt and Pt/Ru anodes in a membrane fuel cell (PEFC). Electrochim Acta 2003; 48(25–26):3899–907.
[50] Danzer MA, Hofer EP. Analysis of the electrochemical behaviour of polymer electrolyte fuel cells using simple impedance models. J Power Sources 2009;190(1):25–33.
[51] Schulz T, Weinmüller C, Nabavi M, Poulikakos D. Electrochemical impedance spectroscopy analysis of a thin polymer film-based micro-direct methanol fuel cell. J Power Sources 2010;195(22):7548–58.
[52] Markovic NM, Ross PN. Surface science studies of model fuel cell electrocatalysts. Surf Sci Rep 2002;45(4–6):121–229.
[53] Maritan A, Toigo F. On skewed ARC plots of impedance of electrodes with an irreversible electrode process. Electrochim Acta 1990;35(1):141–5.